A mobilised bearing capacity approach to the performance-based design of unpaved roads

A.S. Lees [a,b,*], J. Han [c]

[a] Global Application Technology Manager, Tensar International, PO Box 14751, Nicosia 2456, Cyprus
[b] Visiting Research Fellow, University of Southampton, UK
[c] Roy A. Roberts Distinguished Professor, CEAE Department, Univ. of Kansas, 1530 W. 15th St., Lawrence, KS66045-7609, USA

A B S T R A C T

Unpaved roads are used on low traffic or temporary roads such as for materials transport across construction sites or mines. Performance is usually expressed as a rut depth and if it becomes too large, the passage of vehicles may be hindered and repairs needed. A new design method to calculate the required aggregate thickness to avoid excessive rutting both at the surface and at subgrade level is proposed. Tyre size is an input parameter allowing application of the method to a wide range of cases from heavy haul roads to lightly trafficked local roads. A wide range of rut depths and axle passes may be specified, even as low as values typically required in proof roll testing. The proposed method takes a mobilised strength approach to predict permanent deformation on the first pass by means of newly derived hyperbolic relationships. The permanent deformation on the first pass is then coupled with a separately derived deformation accumulation (logistic) function to predict rut depths following the first pass. The adaptation of well-established bearing capacity design methods with fundamental soil strength parameters has provided a framework for the method's application to a wide range of aggregate and subgrade soil types, including low-quality or recycled aggregates as well as those mechanically stabilised by geogrid.

Introduction

Unpaved roads are those constructed of an unbound aggregate layer or layers without a hard surface composed of, for example, asphalt concrete (flexible pavement) or Portland cement concrete (rigid pavement). Therefore, vehicles are supported directly on the unbound aggregate surface. They are often used on low traffic volume or temporary roads such as for the transport of equipment and materials across construction sites or mines.

Performance of an unpaved road is usually expressed as a rut depth and if it becomes too large, the passage of vehicles may be hindered and repairs needed. Excessive deformation also leads to a more rapid deterioration of the road because it can lead to poor drainage resulting from fines migration from the subgrade into the aggregate. Subgrade rutting can lead to water ponding which causes further deterioration of the subgrade (more difficult to repair than surface rutting).

Rutting results from the accumulation of permanent (plastic) deformation in the unbound aggregate and subgrade. When vehicle loads are so low that the elastic limit of the layers is not exceeded, no permanent deformations occur. When the elastic limit is exceeded, permanent deformation accumulates in one of two distinct patterns [35,14,8], as illustrated in Fig. 1:

a) Shakedown: permanent deformation accumulates at a gradually decreasing rate, eventually reaching an equilibrium condition or state of shakedown under a particular loading pattern where no further permanent deformation occurs.
b) Ratcheting: above a shakedown or threshold repetitive load level, permanent deformation accumulates at a rapid or gradually increasing rate towards failure.

The objective of the design method is straightforward: given a wheel load P passing n times along a proposed road, and a subgrade soil of a certain strength (often expressed as a California bearing ratio (CBR) or undrained shear strength), what aggregate layer with thickness H is needed to keep the surface rut depth below a specified level (typically around 40 to 75 mm).

Older design methods to calculate H, such as Powell et al [34] and Giroud and Noiray [16], tended to be empirical and based on a narrow set of observations. They had a single performance or failure criterion (e. g. 75 mm rut depth) and a single standard axle load (e.g. 80 kN). As a result, they did not capture the true mechanics of the problem and had a narrow field of application.

Mechanistic-empirical methods introduced some stress analysis to the problem. The Thompson et al [38] method for mining haul roads uses elastic layer analysis to determine the minimum H value to keep

Notation

B	Width or diameter of loaded area	n_f	Number of axle passes or load repetitions at failure
B_g	Tyre width at road surface for aggregate layer deformation calculation	p	Tyre inflation pressure
B_T	Tyre width at road surface for subgrade deformation calculation	p'_0	Effective overburden pressure on subgrade surface
E_s	Young's modulus of road surface	p_a	Atmospheric pressure at sea level
E_t	Young's modulus of tyre	p_g	Tyre contact stress for aggregate deformation calculation
E_r	Relative stiffness	p_T	Tyre contact stress for subgrade deformation calculation
H	Aggregate layer thickness	q_g	Surface bearing capacity of aggregate only
I_p	Plasticity index	q_s	Surface bearing capacity of subgrade
L	Length of tyre contact area	q_T	Punching shear bearing capacity
M	Mobilisation factor	r	Surface rut depth
M_g	Mobilisation factor on aggregate layer bearing capacity	r_s	Subgrade rut depth
M_T	Mobilisation factor on punching shear bearing capacity	s_u	Undrained shear strength
M_{Tf}	Mobilisation factor on punching shear bearing capacity above which ratcheting deformations occur	s_γ	Bearing capacity shape factor
		α	Normalised shakedown deformation after first loading
N_q	Bearing capacity coefficient for overburden pressure	γ	Shear strain
N_γ	Bearing capacity coefficient for soil self-weight	γ_s'	Effective soil unit weight
P	Wheel load	$\gamma_{M=0.5}$	Reference shear strain at 50 % shear strength mobilisation
P_g	Wheel load used in aggregate layer deformation calculation	δ	Settlement
		δ_p	Permanent surface settlement
P_T	Wheel load used in subgrade deformation calculation	$\delta_{p,n=1}$	Permanent surface settlement when $n = 1$
R	Tyre radius	δ_g	Permanent aggregate layer deformation
R_f	Interface friction ratio between aggregate layer and subgrade	$\delta_{g,n=1}$	Permanent aggregate layer deformation when $n = 1$
		δ_T	Permanent subgrade settlement
T	Load transfer efficiency of aggregate layer for punching shear calculation	$\delta_{T,n=1}$	Permanent subgrade settlement when $n = 1$
		ν_s	Poisson's ratio of road surface
n	Number of axle passes or load repetitions	ν_t	Poisson's ratio of tyre
		φ'	Internal friction angle of aggregate layer
		φ'_{corr}	Internal friction angle of aggregate layer corrected for interface friction with subgrade
		ψ	Dilatancy angle of aggregate layer

subgrade vertical strain below certain levels depending on the designated road category. The empirically derived thickness design curves of the California Procedure [33] were developed in several stages as described by Gonzalez et al. [17] by the US military into a mechanistic-empirical method intended primarily for airfield pavements but often applied in unpaved road design. Elastic stress analysis is used to keep strength mobilisation at the subgrade surface at a constant value with corrections applied for multiple-wheel assemblies and traffic volume. Both of these methods have the disadvantage of having only a single and imprecisely defined performance criterion.

Giroud and Han [15] advanced the State of the Art significantly by introducing a more mechanistic approach that allowed different performance criteria as well as different axle loads and tyre contact areas. However, their design method still required a number of significant assumptions that restricted its use, such as a maximum modulus ratio between the aggregate layer and subgrade, the consideration of permanent deformations in the subgrade only and a linear relationship between subgrade strength mobilization and rut depth.

Powell et al [34] and Giroud and Noiray [16] considered standard axle loads, so the 4th power rule was used to estimate the effect of non-standard axle loads. However, there was no consideration of the effect of vehicle tyres at distributing axle loads to the road surface. Giroud and Han [15] improved this aspect by estimating the tyre contact area and pressure. They assumed the contact stress to be equal to the tyre inflation pressure which was assumed to be applied over a circular contact area of the corresponding radius needed to support the wheel load in equilibrium. The assumption of the tyre contact stress being equal to the tyre inflation pressure works reasonably well on hard surfaces [12] but Lees et al [23] showed that this leads to a significant overestimation of average contact stress on deformable surfaces (unbound aggregate). They measured the tyre contact area between a dual-tyre and unbound aggregate at two different wheel loads combined with two different tyre inflation pressures. The contact width was found to depend on the tyre tread width while the contact length increased with tyre load but was not significantly affected by the tyre inflation pressure. Lees et al [23] derived a calculation method to estimate the average tyre contact stress on unbound aggregate. It assumed a more realistic rectangular shaped contact area of width equal to the tyre width and the length calculated using Hertzian frictionless elastic contact theory. The contact length depends on the tyre radius, tyre load and stiffness properties of the tyre and road surface according to Equation (1). An approximate relationship between tyre stiffness and tyre inflation pressure was derived (Equation (2)) and a reduced stiffness of unbound aggregate of about 12 MPa was adopted to take account of aggregate yield under the high contact stresses. This stiffness is not fixed but varies with aggregate type and quality.
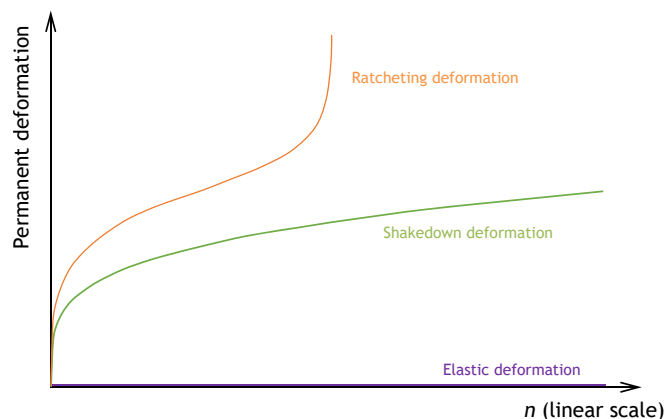
Fig. 1. Modes of deformation accumulation.

$$L = \sqrt{\frac{16RP_g}{\pi E_r B_g}} \tag{1}$$

with $\frac{1}{E_r} = \frac{1-\nu_t^2}{E_t} + \frac{1-\nu_s^2}{E_s}$

$$E_t = 7.4p + 16p_a \tag{2}$$

A new design method for unpaved roads that overcomes some of the shortcomings of existing methods is proposed in this paper. It attempts to faithfully take account of the true mechanics of the problem and, as such, be more widely applicable for a range of subgrade soil types, aggregate types, axle loads, tyre sizes and rut depths. The main motivation for its development was to provide a framework for the design of high to low quality aggregates in road construction, including those mechanically stabilised by geogrid.

Permanent deformation on first loading

Vardanega and Bolton [41] developed a mobilised bearing capacity approach to the prediction of the undrained settlement of circular footings on clay. It took the form of Equation (3) where δ is the settlement which was normalized by the footing diameter B to become dimensionless. δ/B was related to the mobilisation of bearing capacity M expressed as a ratio where 1 denotes full mobilisation and 0 denotes zero mobilisation. The term $\gamma_{M=0.5}$ is the reference shear strain at 50 % shear strength mobilisation in an undrained triaxial compression test and the 1.35 denominator provided a means of relating the average strain in the mobilised mechanism to the ratio of undrained settlement δ to footing diameter B. It was found to give reasonably accurate settlement predictions across typical mobilization levels of about $0.2 < M < 0.8$.

$$\frac{\delta}{B} = \frac{\gamma_{M=0.5}}{1.35}M^{1.67} \tag{3}$$

A similar mobilised bearing capacity approach is proposed to predict the permanent road surface settlement under the first wheel loading but it needs to be applicable at lower mobilization levels of about $0 < M < 0.5$ and for a two-layer supporting system comprising an unbound aggregate and the underlying subgrade. This approach is particularly suited to the prediction of permanent (plastic) deformation which depends primarily on soil strength mobilisation. Lees and Kelly [22] applied this approach successfully to the prediction of subgrade deformation accumulation in their performance-based railway formation design method. They derived a hyperbolic relationship between mobilised subgrade shear strength and permanent strain and between mobilised bearing capacity and permanent deformation, both on the first axle loading, derived from an extensive finite element analysis parametric study.

The proposed approach is illustrated by means of hypothetical plate load test data in Fig. 2. The applied load expressed as a ratio of the load at bearing capacity failure, i.e., the mobilisation ratio M, is plotted against the total (elastic and permanent) plate settlement δ normalised by the plate diameter B. Three unload phases are included at the end of which the elastic deformation is recovered leaving only the permanent deformation. The corresponding permanent deformation is also plotted and forms a similar shape to the total deformation plot. The horizontal distance between them represents the elastic deformation at each load. It is common to represent stress–strain or load–displacement curves such as these as hyperbolic functions [13,31]. With a hyperbolic relationship established between M and normalised permanent deformation δ_p/B, it would be possible to predict the permanent deformation on the first loading if the bearing capacity were known.
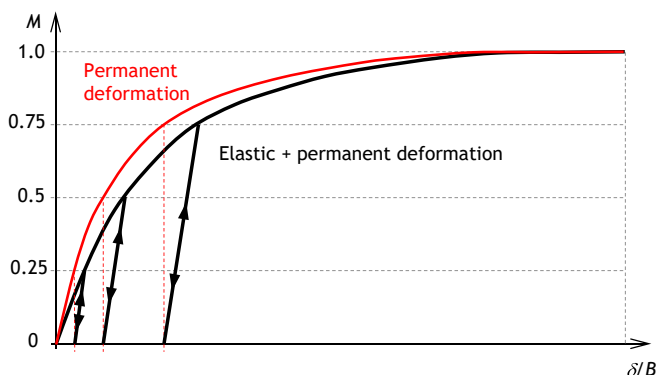
Subgrades and aggregates typically have very different characteristics, so permanent deformations would be expected to accumulate at different rates in each, as demonstrated by Baladi et al [1] and Lees & Tutumluer [24] and described in a subsequent section. Consequently, an improved prediction of surface rutting accumulation should be gained by calculating them separately and then summing them as illustrated in Fig. 3. As well as potentially accounting for the accumulation in each layer more accurately, this has the advantage of explicitly predicting the subgrade rut which is also an important parameter in road design. Excessive rutting in low permeability subgrades can lead to water ponding, deterioration of the subgrade and an acceleration of rutting accumulation. This cannot be rectified simply by filling ruts at the surface but requires expensive and time-consuming reconstruction of the entire road structure.

Permanent subgrade settlement on first loading

Where an aggregate layer overlies a weaker, fine-grained subgrade, punching shear bearing failure would be expected to be more critical than a general shear failure through the aggregate layer and subgrade, as assumed in working platform design [3]. Permanent subgrade settlement results from partial mobilisation of punching shear bearing capacity. Full bearing capacity mobilisation would involve punching shear through the aggregate layer and a bearing mechanism in the subgrade, as illustrated in Fig. 4. The static bearing capacity can be calculated by a two-layer approach, such as Meyerhof [30], but for simpler programming, Lees [21] derived Equations (4) and (5) to determine the punching shear bearing capacity at the surface q_T normalised by the subgrade surface bearing capacity q_s based on the geometric ratio H/B_T and a load transfer efficiency T of the aggregate layer that depends on the strength ratio between the upper and lower layers. It was validated for static bearing capacity using the results of a literature review of centrifuge model testing and numerical analyses [21]. It has also been adapted to include the benefits of mechanical stabilisation in the upper aggregate layer and is used extensively in working platform design.

$$\frac{q_T}{q_s} = 1 + T\frac{H}{B_T} \text{ (strip footing)} \tag{4}$$

$$\frac{q_T}{q_s} = \left(1 + T\frac{H}{B_T}\right)^2 \text{ (square footing)} \tag{5}$$

Fig. 2. Relating mobilised bearing capacity and settlement in a plate load test.
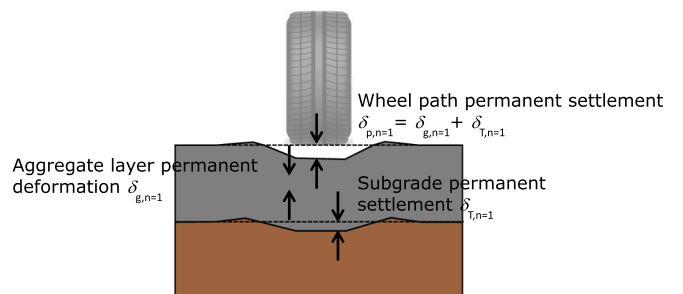
Fig. 3. The two components of permanent surface settlement.
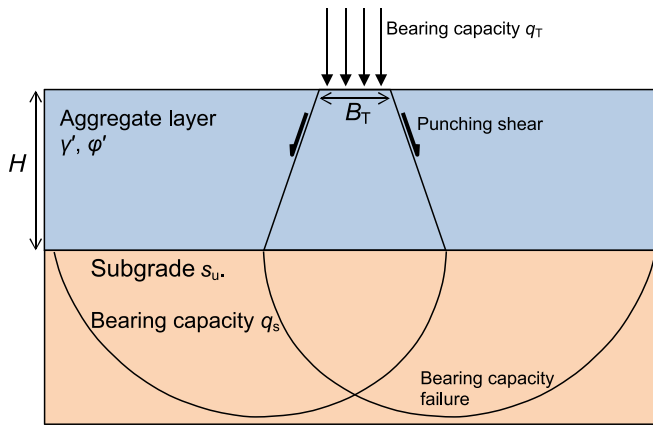
Fig. 4. T-value method to determine punching shear bearing capacity.

The strip ($B_T/L = 0$) and square ($B_T/L = 1$) bearing capacities are calculated using Equations (4) and (5) respectively and then the bearing capacity for any intermediate value of B_T/L obtained by linear interpolation. The loaded width B_T equals the tyre width in single wheel cases but the full dual tyre width in dual wheel cases since the effects of the two tyres merge into one once the load is distributed down through the aggregate layer. q_s is the bearing capacity of the subgrade surface with the same B_T value but no aggregate, calculated according to Equation (6) for undrained subgrades.

$$q_s = (2+\pi)s_u\left(1 + 0.2\frac{B_T}{L}\right) \qquad (6)$$

The T value is determined for undrained subgrade soils using Equation (7) [21] where p'_0 is the effective overburden stress at the base of the aggregate layer.

$$T = 1.4\left(\frac{s_u}{p'_0}\right)^{-0.41\varphi'_1 - 0.18} + 4.2\varphi'_1 - 3.4 \qquad (7)$$

The assumed channelised nature of the wheel loading constrains permanent deformations into a plane strain pattern perpendicular to the direction of wheel travel. As a result, the B_T dimension equals the single or dual tyre width even when this is larger than the tyre contact length, as illustrated in Fig. 5.

Once the punching shear bearing capacity q_T has been calculated, its ratio of mobilisation M_T is determined from Equation (8). The numerator is the average applied pressure from the vehicle tyre which, in turn, is the tyre load P distributed over the contact area, as illustrated in Fig. 5. The contact width approximately equals the tyre width (or total width across both tyres in a dual tyre case) and the contact length can be estimated based on tyre inflation pressure or, preferably, based on Hertzian elastic contact theory using Equations (1) and (2) as described
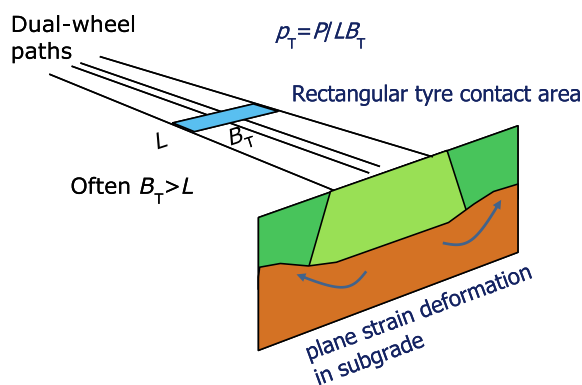
by Lees et al [23].

$$M_T = \frac{p_T}{q_T} = \frac{P/(B_T L)}{q_T} \qquad (8)$$

The hyperbolic function shown in Equation (9) and illustrated in Fig. 6 allows the subgrade permanent settlement $\delta_{T,n=1}$ to be estimated. Such a function allows permanent settlement to be predicted across the full range of mobilisation ratios from zero at the origin to infinity when a mechanism forms at a mobilisation ratio of one. It is necessarily more complex than the log–log expression of Equation (3) which was valid for a narrower range of mobilisation ratio. It has been derived from the back-analysis of cyclic plate load tests and full-scale trafficking tests as presented later in this paper which had fine-grained subgrade soils with a range of I_p values. It is possible that the number in the denominator needs to be adjusted depending on the characteristics of the subgrade soil including plasticity. In their extensive review of clay soil stress--strain behaviour, Vardanega and Bolton [41] found that the strain at 50 % shear strength mobilisation tended to increase with I_p and proposed a relationship, albeit with a high degree of uncertainty. It will be shown later in this paper in the calibration section that Equation (9) provided reasonably accurate outputs for physical tests on fine-grained soils of a range of I_p values. Indeed, the outliers tended to follow an opposite trend with I_p, so there was no reliable indication of a relationship with I_p based on the relatively small dataset. Further testing would be required to investigate the effect of I_p. The threshold shown in Fig. 6 is discussed in the following section on shakedown deformation.

$$\frac{\delta_{T,n=1}}{B_T} = \frac{M_T^{1.5}}{82(1 - M_T)^2} \qquad (9)$$

The advantage of using a hyperbolic relationship is that it should provide a more accurate prediction of settlement across the full range of mobilisation ratios since it begins at the origin and tends towards infinity as the mechanism at $M_T = 1$ is approached. The linear relationship derived by Giroud and Han [15], by comparison, is applicable across a narrow range of mobilisation ratios.

Values of $\delta_{T,n=1}$ can be very small at low M_T values and, if, in reality, the loading remained below the elastic limit, $\delta_{T,n=1}$ would even be zero. Accurate physical measurement of small $\delta_{T,n=1}$ values due to plate or tyre loading would be difficult due to the effects of seating the plate or tyre on the surface. In such cases, it may be determined by curve fitting with the accumulation of deformation under a high number of load repetitions.

Fig. 5. B_T and L conventions in subgrade bearing capacity calculations.
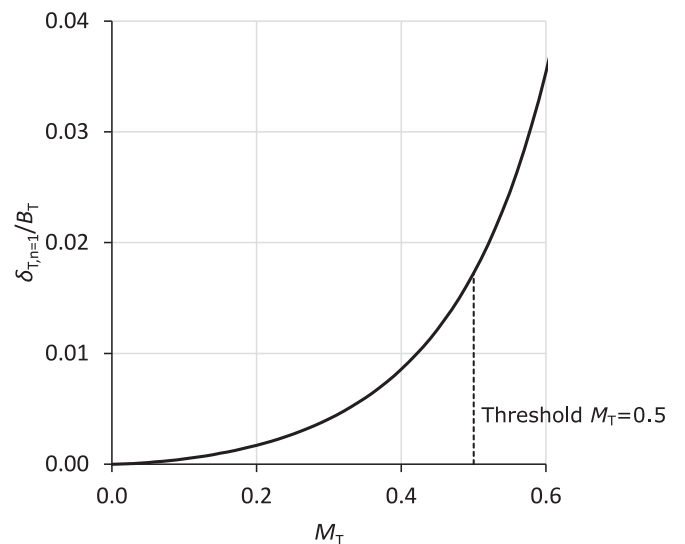
Fig. 6. Proposed hyperbolic relationship between mobilised bearing capacity and permanent subgrade deformation.

Permanent aggregate layer deformation on first loading

A similar approach based on the mobilisation ratio M_g of aggregate layer bearing capacity is proposed for the calculation of the contribution of aggregate layer permanent deformation to surface settlement. This first requires the calculation of the ultimate bearing capacity q_g of the aggregate for the tyre contact area geometry and aggregate shear strength. This is calculated using the Terzaghi [37] bearing capacity equation (Equation (10)). The embedment bearing factor N_q is not required because the tyre load is applied at the surface. Also, the cohesion component is omitted since unbound aggregate does not possess true cohesion and its shear strength is defined here in terms of a secant friction angle φ'.

$$q_g = \frac{1}{2}B_g\gamma_s'N_\gamma s_\gamma \tag{10}$$

The equations for the bearing capacity factor for self-weight density N_γ and the corresponding shape factor s_y commonly used in geotechnical design tend to become inaccurate at the high φ' values typical of road base aggregates. Hence, the Loukidis and Salgado [28] Equations (11) and (12) will be adopted. Equation (11) is valid for cases where the difference between φ' and ψ is 30° which is considered reasonable for most aggregates.

$$N_\gamma = \left(\frac{1 + \sin\varphi'}{1 - \sin\varphi'}e^{(1-0.13\tan\varphi')\pi\tan\varphi'} - 1\right)\tan(1.34\varphi') \tag{11}$$
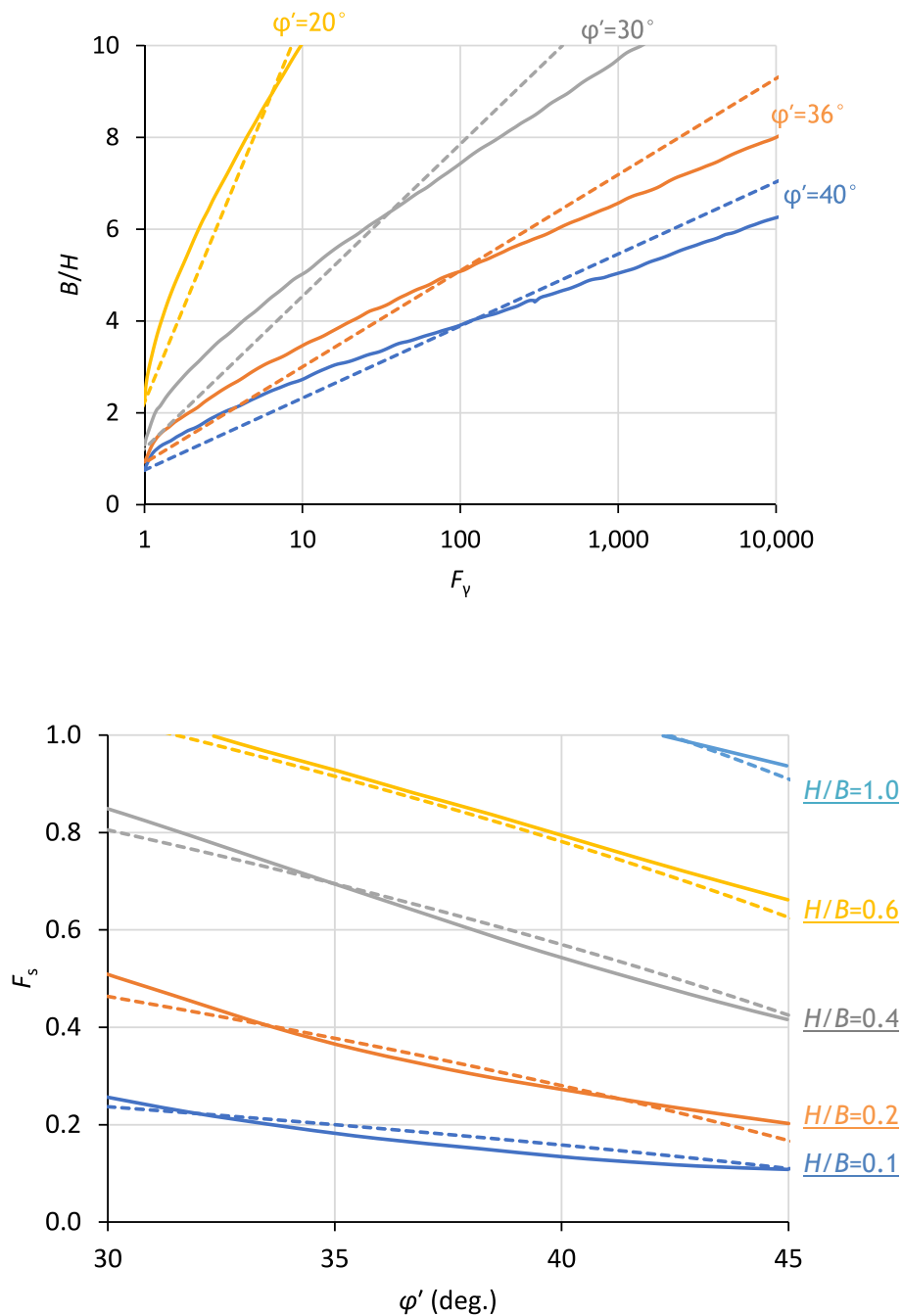
Fig. 7. N_γ and s_y correction factors for thin aggregate layers.

$$s_\gamma = 1 + \left(0.26\frac{1+\sin\varphi'}{1-\sin\varphi'} - 0.73\right)\frac{B_g}{L} \tag{12}$$

The finite thickness of the aggregate layer must be considered since Equations (10)–(12) assume an infinite depth. Meyerhof [30] derived correction factors for N_γ and s_y for a thin sand layer on a rough, rigid base based on the solution for a rough, rigid strip footing derived by Mandel and Salencon [29]. N_γ increases markedly as H/B decreases due to squeezing of the failure mechanism while s_y tends to decrease.

The N_γ and s_y correction factors (F_γ and F_s respectively) were presented in graphical form by Meyerhof [30] and Mandel and Salencon [29] which are redrawn as the solid lines in Fig. 7. These lines were approximated using Equations (13) and (14) for simpler programming and are represented by the dashed lines in Fig. 7. When F_γ is 1, the bearing capacity is not influenced by the aggregate layer thickness and this occurs at H/B values in excess of about 1 for φ' values typical of a road base material. Similarly, F_s stays at 1 once H/B exceeds about 1.

$$F_\gamma = \text{EXP}\left(\frac{\frac{B_g}{H} - 0.6(\tan\varphi')^{-1.3}}{0.48(\tan\varphi')^{-2}}\right), \qquad F_\gamma \geq 1 \tag{13}$$

$$F_s = \left(0.08\frac{B_g}{H} - 1.1\right)\tan\varphi' - 0.66\ln\left(\frac{B_g}{H}\right) + 1.93, \quad F_s \leq 1 \tag{14}$$

The Meyerhof [30] approach assumed a rough bottom boundary to the aggregate layer whereas aggregate layers constructed on weak, fine-grained subgrade soils are unlikely to benefit from a rough interface. Anything less than a fully rough interface would result in a reduced bearing capacity when the bottom boundary is shallow enough to influence bearing capacity. Chang et al [7] undertook 150 mm diameter plate load tests on a 50, 100 or 150 mm thick layer of dry, uniform Kansas River sand (φ'=38.6°, γ_s=17.84 kN/m³) supported by a rigid bottom boundary with different materials placed on top including wood, steel, concrete and geosynthetics. The interface friction between the sand and bottom boundary materials was determined separately in direct shear tests and expressed as a ratio R_f of the sand's internal friction angle. R_f ranged between 0.45 for steel, 0.70 for wood and concrete and as high as 0.88 for geosynthetics. They showed that bottom boundaries with lower frictional properties caused a reduction in measured bearing capacity and the effect was greater when the bottom boundary was shallower.

Using the Chang et al [7] test data as a guide, a correction to the aggregate layer φ' value was derived to take account of both the reduced interface friction R_f at the bottom boundary of the aggregate layer and the proximity of the bottom boundary to the surface loading expressed as the ratio H/B as shown in Equation (15). The interface friction has an exponentially increasing influence as it comes closer to the surface loading. When H/B is sufficiently large, the interface friction has no influence on bearing capacity. This happens when H/B is approximately 1 but increases with aggregate layer strength, hence φ' needs to be corrected (in radians) with the exponential in Equation (15).

$$\varphi'_{\text{corr}} = \varphi'\left[1 - \left(1 - R_f\right)\left(2.5e^{-\frac{\pi}{\varphi'}\frac{H}{B_g}}\right)\right], \quad \varphi' \geq \varphi'_{\text{corr}} \geq 0 \tag{15}$$

The Chang et al [7] measured bearing capacity values in all the plate load tests are compared in Fig. 8 with values determined using Equations (10)–(14) with the φ' value corrected according to Equation (15). The red symbols denote R_f values of between 0.83 and 0.88, the gold symbols between 0.70 and 0.73 and the blue symbols an R_f value of 0.45. The match is very good for the higher two H/B ratios while for H/B = 0.33 the average match is good but there was higher scatter due to the closer proximity of both the top and bottom boundary conditions and high sensitivity to the R_f value.

Equations (10)–(15) are used in the calculation of q_g. The R_f value is the ratio of shear strengths between the aggregate layer and the subgrade. Since shear strength in the aggregate layer is frictional and stress-
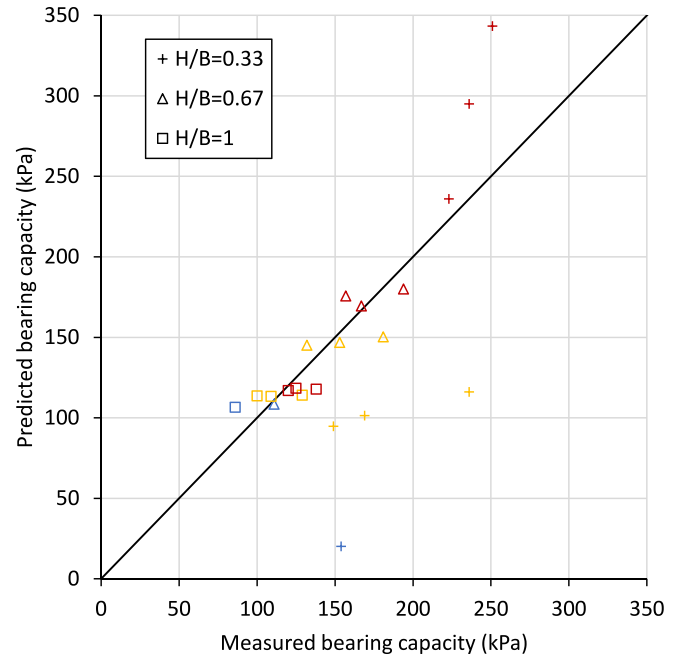
Fig. 8. Comparison between measured and predicted values of bearing capacity of thin sand layers overlying bottom boundaries of different interface friction.

dependent, the normal stress at the interface is estimated using an approach such as that shown in the shakedown deformation worked example in this paper. As for the subgrade, aggregate layer deformations are constrained into a plane strain pattern perpendicular to the direction of wheel travel. As a result, the B_g dimension equals the tyre width even when this is larger than the tyre contact length, as illustrated in Fig. 9. The B dimension is given the subscript g to distinguish it from the B_T value adopted in subgrade deformation calculations which will differ in dual wheel cases since the full dual-wheel width is adopted for the calculation of δ_T and the individual tyre width for δ_g.

M_g is calculated from Equation (16) using q_g calculated from Equations (10)–(15), and p_g as shown in Fig. 9 from the wheel load P.

$$M_g = \frac{p_g}{q_g} = \frac{P/(B_gL)}{q_g} \text{ (single wheel) or } \frac{P/(2B_gL)}{q_g} \text{ (dual wheel)} \tag{16}$$

The hyperbolic relationship shown in Equation (17) and illustrated in Fig. 10 allows the component of aggregate layer deformation $\delta_{g,n=1}$ that contributes to permanent surface settlement to be estimated. It has been derived from the back-analysis of cyclic plate load tests and full-scale trafficking tests on typical road base aggregates as presented later in this paper. The value 1.05 instead of 1.0 appears in the denominator in recognition of the fact that even when the bearing capacity of the aggregate layer is fully mobilised ($M_g = 1$), a mechanism does not
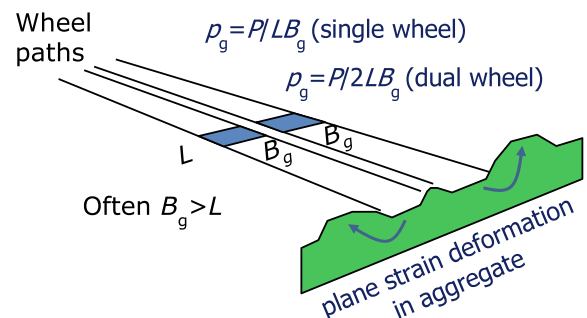
Fig. 9. B_g and L conventions in M_g calculations.
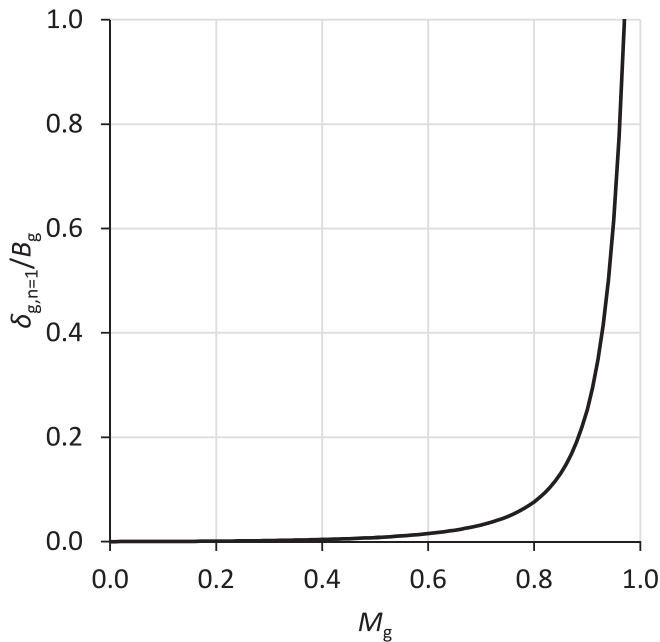
Fig. 10. Hyperbolic relationship between mobilised bearing capacity and permanent aggregate layer deformation.

form because as a wheel sinks into the aggregate its contact area increases and hence the contact stress reduces.

$$\frac{\delta_{g,n=1}}{B_g} = \frac{M_g^{1.5}}{150\left(1.05 - M_g\right)^2} \tag{17}$$

As with $\delta_{T,n=1}$ and M_T, values of $\delta_{g,n=1}$ can be very small at low M_g values and, if, in reality, the loading remained below the elastic limit, $\delta_{g,n=1}$ would even be zero. Accurate physical measurement of small $\delta_{g,n=1}$ values due to plate or tyre loading would be difficult due to the effects of seating the plate or tyre on the surface. In such cases, it may be determined by curve fitting with the accumulation of deformation under a high number of load repetitions.

Shakedown permanent deformation accumulation

Below a certain threshold loading, permanent deformation accumulates at a gradually decreasing rate, eventually reaching an equilibrium condition or state of shakedown under a particular loading pattern where no further permanent deformation occurs. The threshold stress is often expressed as a ratio of the peak cyclic deviatoric stress q_c to the peak deviatoric stress q_f in a static triaxial test of the same initial stress state and stress history or, in other words, in terms of a strength mobilisation factor. Values quoted in the literature range from about 0.67 [36] to 0.6 [25] and 0.55 [45] in fine-grained soils subjected to low numbers of cycles at the same strain rate as the static test to failure. For granular soils, a value of around 0.67 has been suggested [4] but a single ratio may be an over-simplification for granular soils. Lekarp and Dawson's (1998) repeated load laboratory tests did not support such a relationship, Arnold et al (2002) found that the threshold stress of only certain aggregates could be defined in this way and Werkmeister et al (2001) found that such ratios tended to vary across a range. The strength ratio for fine-grained soils could be expressed similarly in terms of a failure mechanism mobilisation ratio, e.g., mobilised bearing capacity as illustrated in Fig. 2.

For high-plasticity clay subgrades, a threshold subgrade bearing capacity mobilisation of 0.5 has been set, as illustrated in Fig. 6, but this could be adjusted by the designer. Therefore, the permanent deformation accumulation function described in this section is applied to

subgrade permanent deformation accumulation only when M_T is at 0.5 or below. A threshold load for the aggregate layer is considered less important for wheel loads because any sinking causes the contact area to increase and contact stress to decrease.

Lees and Tutumluer [24] performed a review of cyclic and repeated load triaxial tests to a high number of cycles on a range of soil types including clay, silt, sand, rail ballast and rail sub-ballast. They proposed the shakedown deformation accumulation function shown in Equation (18) and plotted in Fig. 11. With just one input parameter α, it was possible to characterise the permanent deformation accumulation in the various coarse and fine-grained soils included in the review following the first load cycle all the way to shakedown. It expresses the accumulated permanent deformation as a dimensionless ratio of the permanent deformation occurring on the first loading, $\delta_{p,n=1}$. Consequently, it provides a framework to predict settlement accumulation in both the aggregate and subgrade layers in the design method proposed in this paper. The $\delta_{p,n=1}$ value is determined using the method described in the previous section while only the α parameter is needed to determine the accumulation of deformation in each layer according to Equation (18).

$$\frac{\delta_p}{\delta_{p,n=1}} = \frac{1 + \alpha}{1 + \alpha e^{-0.2\ln n}} \tag{18}$$

Lees and Tutumluer [24] derived the α values shown in Table 1 from cyclic triaxial tests on various soils and other reviews of cyclic testing on soils including the Li [26] study of cohesive subgrade soils. α represents the normalised permanent deformation needed following the first load to reach the shakedown condition. A good fit with experimental data was achieved by setting the maximum rate of deformation accumulation with respect to $\ln n$ to occur when half of α had accumulated, with the number of load repetitions required to reach that point equal to α^5. The resulting functions are compared graphically in Fig. 12. It is apparent that the accumulation of deformation following the first loading broadly increases with decreasing soil particle size and increasing plasticity. Similarly, the number of load repetitions needed to approach shakedown is significantly less for the granular soils than the fine-grained soils.

Calibration of proposed design method

The hyperbolic relationships between mobilised bearing capacity and permanent settlement on first loading in Equations (9) and (17) were determined from the back-analysis of full-scale field trials and experiments. That back-analysis is presented in this section. As well as a calibration of these equations, a comparison with all the physical data as a whole provides a means to assess the reliability of the proposed design method which is a combination of Equations (9) and (17) with the deformation accumulation function described in the previous section. In most cases only the surface settlement accumulation was recorded so it
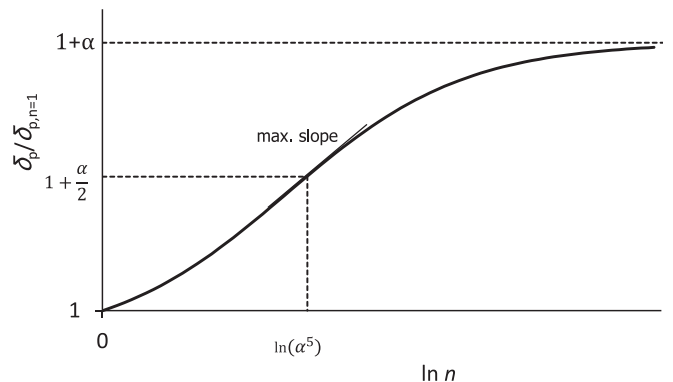
Fig. 11. Function to predict the accumulation of permanent shakedown deformations in soils.

Table 1

Example input parameters to permanent deformation accumulation model [24].

Soil type	Ballast	Sub-ballast or road base	Sand	Plastic clay (CH)	Low-plasticity clay (CL)	Plastic silt (MH)	Non-plastic silt (ML)
α	1.9	3.6	3.2	25	11	5.0	2.5
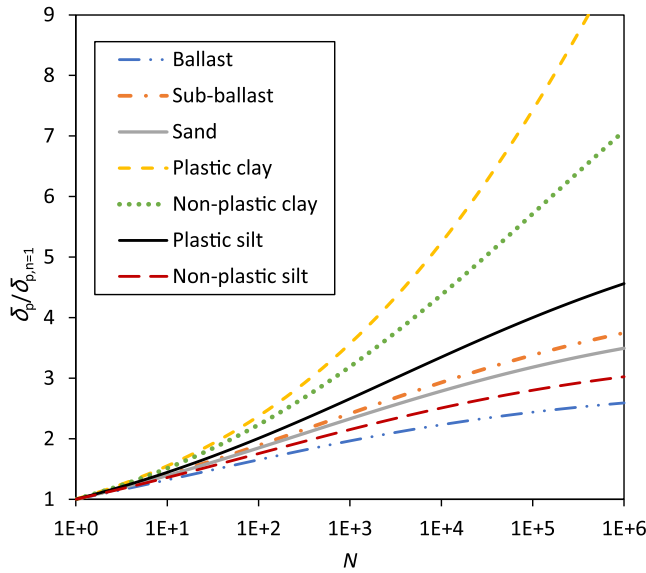
Fig. 12. Comparison of permanent deformation accumulation function parameters derived for different soils [24].

was not possible to calibrate Equations (9) and (17) directly but rather the sum of the subgrade and aggregate layer deformations to obtain the surface settlement.

A literature review was undertaken to obtain full-scale physical test data of the accumulation of permanent deformation in aggregate layers overlying weaker subgrade soil subjected to either rolling pneumatic tyre load or cyclic plate load. Cases with a mobilised subgrade bearing capacity M_T exceeding 0.5 were excluded here but considered in the calibration of the ratcheting deformation accumulation cases described in a later section of this paper.

The suitable studies involving channelised trafficking that provided 12 sets of data altogether are summarized in Table 2. The aggregates were mostly similar in nature and an E_s value of 12 MPa was adopted for the tyre contact area calculation and a φ' value of 45° for the bearing capacity calculations. Higher values of 15 MPa and 46° respectively were adopted for the Little [27] aggregate to allow for mechanical ageing effects since the road was left for a year following construction

prior to trafficking. Lower values of 7 MPa and 43° respectively were adopted for the Yang et al [44] aggregate since it had a lower maximum particle size of 20 mm. The α value for sub-ballast or road base in Table 1 was adopted in the calculation of deformation accumulation according to Equation (18). The tyre widths and radii are shown in Table 2 together with the tyre contact lengths estimated according to the method described by Lees et al [23].

In all cases the subgrade CBR was provided and this was converted to s_u using Equation (19). It is a modification of the $s_u = 23$CBR correlation proposed by Black [2] for over-consolidated clays commonly used in road design, avoiding the over-prediction of s_u at higher CBR values. This puts Equation (19) closer to the correlation proposed by Jenkins and Kerr [18] for Boulder Clay.

$$s_u = 23(\text{CBR})^{0.8} \tag{19}$$

The suitable studies involving cyclic plate load tests provided 10 sets of data altogether and are summarized in Table 3. An advantage of the proposed design method is that permanent settlement accumulation due to both cyclic plate load tests and trafficking can be compared using the same framework due to the higher precision of the Lees et al [23] approach to considering tyre contact areas. The aggregates suitable as a road base or sub-base layer were assigned a φ' value of 45°. The Palmeira and Antunes [32] study used a gravel with a low fines content so a higher φ' value of 47° was adopted. One set-up in the Cote [10] study used a thick layer of medium to coarse sand instead of road base for which a lower φ' value of 43.7° – rather high for a sand but the minimum value to avoid immediate bearing capacity failure – was adopted and the α value adjusted appropriately.

The design calculation procedures proposed earlier in the previous two sections of this paper were followed to derive predicted permanent surface settlement δ_p after 1,000 and 10,000 cycles. The outputs of these calculations are plotted in Fig. 13 and compared with the physically measured values. Given the inevitable variations between tests undertaken on different materials with different equipment and methods, the match between the measured and predicted values is remarkably good and provides greater confidence in the proposed design method's predictions.

The trafficking data matches particularly well, except for the Klopmaker et al (2020) cases as highlighted in Fig. 13. The nature of the manufactured subgrade soil (silty sand) made its strength highly sensitive to moisture content changes and being located outside, exposed to changing weather conditions, would have made the subgrade CBR very

Table 2

Literature review of trafficking trials with M_T less than 0.5.

Source	Tingle & Webster [40]	Little [27]	Yang et al [44]	Cuelho et al [11]	Klopmaker et al [20]	Watts et al [42]
Lab. or field	Lab.	Field	Lab.	Field	Field	Lab.
Aggregate characteristics	Well-graded crushed limestone	UK Type 1 and Sand & Gravel	Sandy gravel 0–20 mm	Crushed aggregate	Crushed rhyolite and diabase	UK Type 1 crushed granite
H (m)	0.508	0.58, 0.428, 0.394	0.24, 0.18	0.632	0.42, 0.5	0.6, 0.46, 0.3
Subgrade characteristics	Plastic clay, I_P 0.51	Soft plastic clay, I_P 0.2 to 0.33	Clay, I_P unknown	Clay, I_P unknown	Silty sand, I_P 0.11	Plastic silty clay, I_P ~ 0.5
Subgrade CBR	0.7	4.6	4.8, 5.4	1.75	2.0, 1.5	2.33, 2.15, 1.99
Subgrade α	25	25	25	25	2.5	25
Tyre width and radius (m)	0.22, 0.51 (dual)	0.195, 0.48 (dual)	0.23, 0.50 (dual)	0.219, 0.53 (dual)	0.3, 0.56 (dual)	0.295, 0.52 (dual)
Wheel load (kN)	37	40	40	37.7	50	40
B_g, B_T and tyre contact length (m)	0.22, 0.6, 0.209	0.195, 0.51, 0.226	0.23, 0.55, 0.241	0.219, 0.454, 0.214	0.3, 0.66, 0.219	0.295, 0.7, 0.183
n	2,000	1,200	5,000	1,600	840, 266	10 k, 10 k, 1.5 k

Table 3

Literature review of cyclic plate load tests with M_T less than 0.5.

Source	Palmeira & Antunes [32]	Cote [10]	Tingle & Jersey [39]	White [43]
Lab. or field	Lab.	Lab.	Lab.	Lab.
Aggregate characteristics	Gravel (low fines)	Well-graded gravel, medium to coarse sand	Well-graded crushed limestone	Well-graded gravel (0–20 mm)
φ' for bearing capacity	47°	45°, 43.7°	45°	45°
Aggregate α	3.6	3.6 or 3.2 (sand)	3.6	3.6
H (m)	0.2	0.409, 0.503, 0.455, 0.909 (sand)	0.51	0.203
Subgrade characteristics	Silty clay, I_p 0.23	Clay, I_p 0.15	Plastic clay, I_p 0.56	Silt and sand, I_p 0.08
Subgrade CBR	8	2.7, 2.9, 2.0, 2.6	1.2	1.8
Subgrade α	25	25	25	2.5
Plate dia. (m)	0.3	0.305	0.305	0.305
Peak load (kN)	40	40.3	39.2	1.57, 4.14, 7.06, 9.12
n	30 k	10 k, 1.2 k (sand)	1 million	166 k
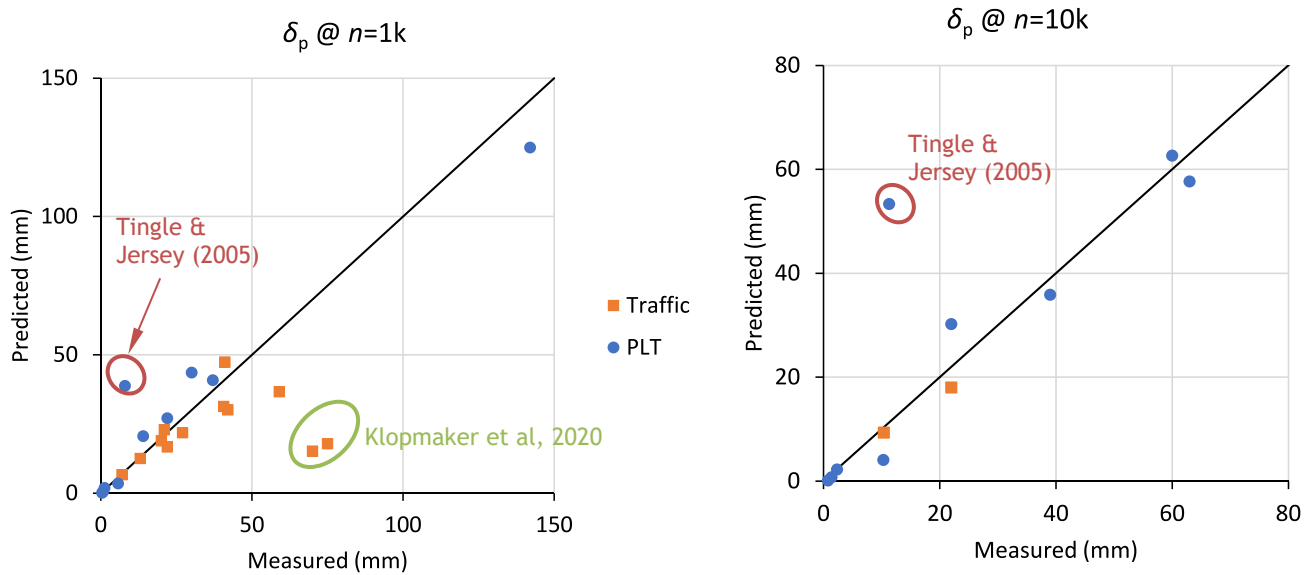
Fig. 13. Comparison of the proposed design method against measured trafficking and cyclic plate load test data from the literature review.

variable and difficult to control. Therefore, only a slight increase in the moisture content of the subgrade would account for the higher-than-expected measured deformation. The cyclic plate load test data also matches well, with the exception of the Tingle and Jersey [39] data. This is likely due to the conditioning sequence of 10 cycles at 4.4 kN increments up to a maximum of 44.5 kN – higher than the peak load in the subsequent load cycling – whose settlements were excluded from the measured data.

Converting wheel path settlement to rut depth

Bearing capacity mobilisation can be related to permanent settlement as described in the previous sections. However, rut depth is a more

common and more useful performance criterion because this affects the trafficability of a road and the distinction between the two is illustrated in Fig. 14. Rut depth also makes a more suitable performance criterion for the subgrade because this directly corresponds with the water ponding depth that may occur. However, direct estimation of rut depth is more difficult because it depends on both the settlement under the wheel path and the heave that occurs to the sides of the wheel path due to shear deformation.

About 100 data points from post-test surveys of surface settlement and rut depth of full-scale trafficking trials are plotted in Fig. 15. The trials were undertaken at the UK Transport Research Laboratory (TRL) [9,42] using a 40-tonne dual wheel heavy vehicle simulator (HVS) passing in a channelised fashion up to 10,000 times over a 0.25 to 0.6 m
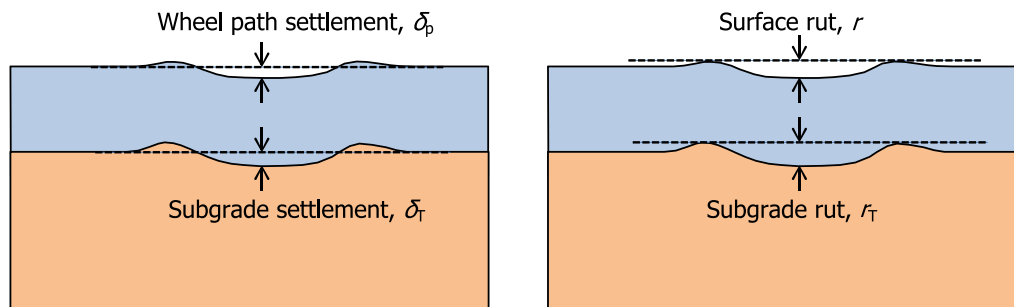
Fig. 14. Distinguishing between settlement and rut depth.
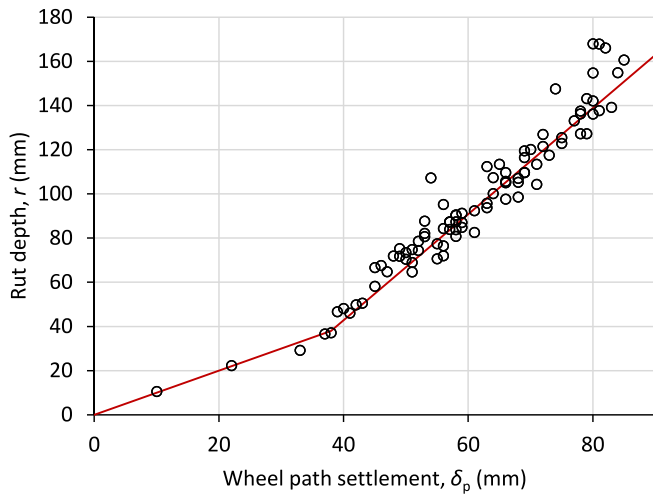
Fig. 15. Measured surface settlement and rut depth from TRL trafficking tests.

thick layer of well-graded crushed limestone overlying a plastic clay subgrade of CBR 1.5 to 2.5 %. It is apparent that settlement and rut depth were about equal up to 38 mm because larger settlements were needed for the heave to develop on each side to cause deeper ruts. As settlements increased beyond 38 mm, the rut depth increased at about 2.4 times the settlement rate due to the combined wheel-path settlement and heave to the sides. The best fit line drawn obeys Equation (20) and could be used to convert calculated settlement into rut depth for similar conditions to these trafficking trials. Since TRL post-test subgrade profiles were measured to be similar to road surface profiles, rut depth development at the subgrade surface would be expected to develop in a similar pattern and the same relationship could be used to convert subgrade settlement into rut depth.

$$r = \delta_p \, (\delta_p \le 38\text{mm}), \, r = 2.4\delta_p - 53.2 \, (\delta_p > 38\text{mm}) \tag{20}$$

Permanent deformation accumulation (shakedown) calculation example

Input data.

Wheel load and tyre contact parameters: $R = 500$ mm, $p_t = 800$ kPa, $B_T = 600$ mm, $B_g^\S = 255$ mm, $L = 178$ mm, $P_T = 36$ kN, $P_g^\S = 18$ kN, $n = 10{,}000$.
Subgrade properties: plastic clay (CH), $\alpha = 25$, $s_u = 55$ kPa
Road properties: hard, crushed rock aggregate of typical road base or sub-ballast grading, $\alpha = 3.6$. $H = 250$ mm, $E_s = 12$ MPa, $\varphi' = 45°$, $\gamma_s' = 20$ kN/m^3.

Calculation

Tyre contact stress distributed to top of subgrade (assuming 2:1 load spread) = 36 kN/[(0.6 + 0.25) * (0.178 + 0.25)] = 99.0 kPa.
$p'_0 = 0.25$ m * 20kN/m^3 = 5 kPa.
Normal stress on subgrade = 99 + 5 = 104 kPa.
Approximate aggregate layer shear strength at interface = 104 * tan 45° = 104 kPa
$R_f = 55/104 = 0.53$
$\varphi'_{corr} = 45° * [1-(1-0.53)*(2.5 \, \text{EXP}(-4 * 0.25/0.255)] = 45° * 0.977 = 44.0°$ (Equation (15))
$F_\gamma = 2.40$ (Equation (13)).
$F_s = 0.899$ (Equation (14)).
$N_\gamma = 2.40 * 128.0$ ($F_\gamma *$ Equation (11)) = 307.2, $s_\gamma = 0.899 * 2.02 = 1.81$ ($F_s *$ Equation (12))

$q_g = 0.5B_g\gamma'_s N_\gamma s_\gamma = 0.5 * 0.255 * 20 * 307.2 * 1.81 = 1418$ kPa (Equation (10))
$M_g = [18 / (0.255 * 0.178)] / 1418 = 0.280$ (Equation (16))
$\delta_{g,n=1}/B_g = 0.148 / 88.9 = 0.0017$ (Equation (17))
$\delta_{g,n=1} = 0.0017 * 255$ mm = 0.4 mm.
$p'_0 = 5$ kPa. $T = 0.319$ (Equation (7))
$q_s = 282.7$ kPa (strip load) or 339.2 kPa (square load) (Equation (6)).
$q_T = 282.7 * (1 + 0.319 * (0.25 / 0.6)) = 320.3$ kPa (strip load) (Equation (4))
$q_T = 339.2 * (1 + 0.319 * (0.25 / 0.6))^2 = 435.4$ kPa (square load) (Equation (5))
Extrapolate for $B_T/L = 3.37$: $q_T = 708.2$ kPa.
$M_T = [36 / (0.6 * 0.178)] / 708.2 = 0.476$ (Equation (8))
$\delta_{T,n=1}/B_T = 0.328 / 22.5 = 0.0146$ (Equation (9))
$\delta_{T,n=1} = 0.0146 * 600$ mm = 8.7 mm.
Permanent surface settlement on first loading $\delta_{p,n=1} = 0.3 + 8.7 = 9$ mm.

Settlement accumulation:

$\delta_g/\delta_{g,n=1} = 4.6/1.57 = 2.93$ (Equation (18))
$\delta_T/\delta_{T,n=1} = 26/4.96 = 5.24$ (Equation (18))
$\delta_g = 2.93 * 0.4$ mm = 1.2 mm
$\delta_T = 5.24 * 8.7$ mm = 45.6 mm

Output.

Accumulated surface settlement $\delta_p = 1.2 + 45.6 = 46.8$ mm ≈ 47 mm.
Accumulated subgrade settlement $\delta_T = 45.6$ mm ≈ 46 mm.
Accumulated surface rut = 2.4 * 46.8 – 53.2, $r = 59$ mm (Equation (20)).
Accumulated subgrade rut = 2.4 * 45.6 – 53.2, $r_T = 56$ mm (Equation (20)).

Notes.

$\S$ - This example has a dual tyre so B_g equals the tyre width and B_T equals twice the tyre width plus the gap between the tyres. Also, P_g is half the dual wheel load while P_T is the total dual wheel load. In a single tyre case, $B_T = B_g$ which is the tyre width and $P_T = P_g$.

Ratcheting permanent deformation accumulation

The surface settlement accumulation recorded in 7 trafficking tests to failure at the TRL test facility with the HVS are shown in Fig. 16. Also in
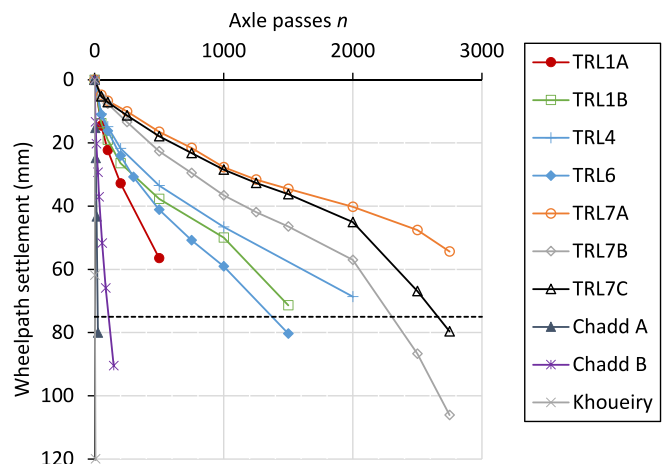
Fig. 16. Deformation accumulation in high M_T cases.

Fig. 16 are shown two sets of results from an earlier trial at TRL by Chaddock [6] using a driven truck and one smaller scale trial by Khoueiry [19]. The parameters of each trial are summarised in Table 4. The subgrade bearing capacity mobilization factor M_T in each case was in the range 0.42 to 1.0 and most of the tests reached the commonly used failure criterion of 75 mm wheel path settlement. The Khoueiry [19] trial did this in a little over one pass, the Chaddock [6] trials in less than 100 passes while the TRL trials took up to about 4,000 passes. Some of the tests, most notably the TRL7 series, exhibited an increasing rate of settlement accumulation towards the end characteristic of the ratcheting deformation form of failure that can occur when M_T exceeds the threshold value typically set at 0.5.

Restricting all unpaved road designs to M_T values below the threshold is considered overly conservative for cases with small (less than 2,000) numbers of axle passes. As shown in Fig. 16, the TRL cases which had M_T values of around 0.5 still supported about 1,000 wheel passes on average before the surface settlement reached 40 mm, and most cases exceeded 2,000 wheel passes before the 75 mm failure criterion was reached. Allowing a limited degree of ratcheting deformation in the subgrade may allow more economical designs on temporary roads with relatively low n values.

As with the shakedown deformation accumulation cases described earlier in this paper, it is useful to normalise the surface settlement by the tyre width. This requires the failure criterion to be defined in terms of a normalised surface settlement too. BSI [5] defines a failure criterion of 0.15 times plate diameter in cases where plate load tests do not reach a clear failure plateau. Adopting the same ratio together with the tyre width B_T appropriate for subgrade deformations (since ratcheting failure would be expected to occur predominately in subgrades rather than the aggregate layer) gives failure surface settlement values of 105 mm in the TRL trials, 85 mm in the Chaddock [6] trials and 30 mm in the Khoueiry [19] test.

Plotting the Fig. 16 data in a different way as the number of passes needed to reach the failure criterion of $0.15B_T$ against M_T as shown in Fig. 17, it is easier to visualise the performance of unpaved roads with high M_T values. Some tests required extrapolation of the data to estimate the n value at failure. It is apparent that full bearing capacity mobilization ($M_T = 1$) results in the failure criterion being reached on just one pass, as would be expected, while the number of passes needed to reach failure increases exponentially as M_T decreases towards the threshold value M_{Tf} as shown by the line defined by Equation (21). Equation (21) takes this form so that n_f equals 1 when M_T equals 1 and so that n_f increases rapidly as M_T falls below the threshold (M_{Tf}). The parameters were selected to achieve a moderately conservative fit to the relatively small number of data points.

$$n_f = M_T^{-2.21} e^{3.21 M_{Tf}} \tag{21}$$

Surface settlement accumulation due to ratcheting deformations of the subgrade may reasonably be approximated as linear from zero at $n = 0$ to the failure criterion of $\delta_T/B_T = 0.15$ at the number of passes needed to reach the failure criterion n_f. This leads to Equation (22), which,

Table 4
Literature review of trafficking trials with M_T greater than 0.5.

Source	Watts et al [42]	Chaddock [6]	Khoueiry [19]
Aggregate characteristics	UK Type 1 crushed granite	UK Type 1 crushed limestone	Poorly graded sandy gravel
H (m)	0.288 to 0.331	0.265, 0.315	0.229
Subgrade characteristics	Plastic silty clay, $I_p \sim 0.5$	Plastic silty clay, I_p 0.38	Clayey sand
Subgrade CBR	1.35 to 2.18	1.6	2
Tyre width (m)	0.295 (dual)	0.229 (dual)	0.2 (solid)
Wheel load (kN)	40	40	28
B_T and tyre contact length (m)	0.7, 0.173	0.57, 0.187	0.2, 0.336
n	Up to 2.5 k	25, 147	1.2 k
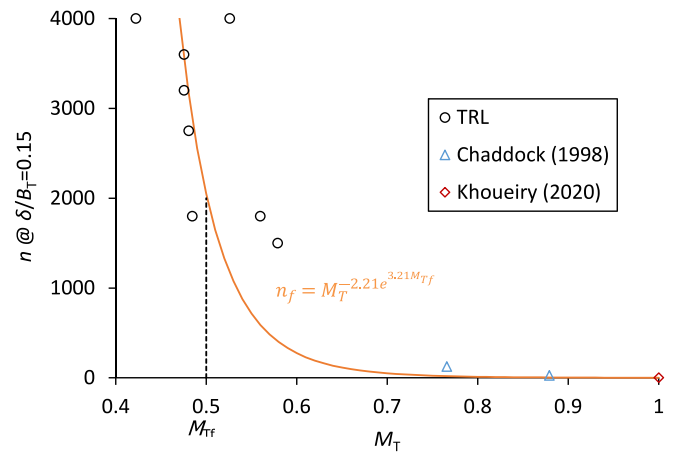
Fig. 17. Unpaved road performance in high M_T cases.

combined with Equation (21), gives the prediction of surface settlement for ratcheting deformations in the subgrade shown in Equation (23). This can provide a design for n values below 2,000 when M_T is above the threshold value M_{Tf}, taken as 0.5 here, but could be adjusted.

$$\frac{n}{n_f} = \frac{\delta/B_T}{(\delta/B_T)_f} \tag{22}$$

$$\frac{\delta_T}{B_T} = \frac{0.15n}{M_T^{-2.21} e^{3.21 M_{Tf}}} \tag{23}$$

Permanent deformation accumulation (ratcheting) calculation example

Input data.

Wheel load and tyre contact parameters: $R = 400$ mm, $B_g = 250$ mm, $B_T = 600$ mm (dual-tyre), $L = 180$ mm, $P_g = 20$ kN, $P_T = 40$ kN, $n = 300$.
Subgrade properties: plastic clay (CH), $s_u = 40$ kPa, $M_{Tf} = 0.5$.
Road properties: hard, crushed rock aggregate of typical road base or sub-ballast grading $H = 400$ mm, $E_s = 12$ MPa, $\varphi' = 43°$, $\gamma_s' = 20$ kN/m³.

Calculation

$p'_0 = 0.4$ m * 20kN/m³ = 8 kPa. $T = 0.389$ (Equation (7))
$q_s = 205.6$ kPa (strip load) or 246.7 kPa (square load) (Equation (6)).
$q_T = 205.6 * (1 + 0.389 * (0.4 / 0.6)) = 258.9$ kPa (strip load) (Equation (4))
$q_T = 246.7 * (1 + 0.389 * (0.4 / 0.6))^2 = 391.7$ kPa (square load) (Equation (5))
Extrapolate for $B_T/L = 3.33$: $q_T = 701.1$ kPa.
$M_T = [40 / (0.600 * 0.180)] / 701.1 = 0.528$ (Equation (8))
$\delta_T/B_T = 45 / 1125 = 0.04$ (Equation (23))
$\delta_T = 0.04 * 600$ mm = 24.0 mm.

Output.

Accumulated surface settlement $\delta_p = 24$ mm (assuming all deformation occurs in subgrade)
Accumulated surface rut $r = \underline{28\text{ mm}}$ (Equation (20)).

Deriving the design equations for new soil types

The design equations to the proposed unpaved roads design method presented in this paper have been calibrated for high quality, hard,

crushed rock aggregates of standard road base gradings on fine-grained subgrade soils. The calibration was performed by back-analysis of a large number of full-scale cyclic plate load test and trafficking trials in such conditions.

Many of the design equations use common soil parameters, such as shear strength and unit weight, which can be determined by standard tests. This significantly facilitates the introduction of other aggregate and subgrade soil types into the proposed design method. Some of the design equations do not contain common soil parameters and approaches to introduce other soil types are discussed in the remainder of this section.

Hyperbolic relationships

The hyperbolic relationships (Equations (9) and (17)) form an important part of the proposed design method. They relate the mobilisation of bearing capacity to the permanent settlement on the first axle pass. Equation (9) was calibrated using data from fine-grained subgrades with I_p values ranging from 0.08 to 0.56. Vardanega and Bolton [41] noted that a higher plasticity index increased the predicted settlement of footings loaded directly on clay soils when taking a mobilised bearing capacity design approach. However, the physical test data used in the calibration of Equation (9) did not exhibit this trend, or even an opposite trend for the small number of cases at each I_p value. Equation (9) provided a reasonably accurate prediction for most cases in the calibration exercise for a range of fine-grained subgrade soils. Designers could opt to derive hyperbolic equations for specific subgrade soils, including granular soils, using laboratory or field tests with unload-reload loops in order to determine the relationship between strength or bearing capacity mobilisation and permanent deformation. Any new relationship should be validated by cyclic plate load tests or trafficking trials with measurement of subgrade settlement accumulation.

Equation (17) was calibrated using data for typical road aggregates. It is hard to assess how accurate this equation would be for other aggregates. Therefore, in a similar fashion to new subgrade soil types, new hyperbolic relationships would need to be derived for alternative aggregate types and validated by cyclic plate load tests and trafficking.

Deformation accumulation (shakedown) α value

Equation (18) provides a framework for the prediction of settlement accumulation with axle load repetitions in most soil types. Soils are characterised in terms of the α value and example values derived by Lees and Tutumluer [24] are shown in Table 1. These may be used to estimate settlement accumulation. Aggregate and subgrade soil-specific α values may be derived by cyclic triaxial testing at a range of stress states to a sufficiently high number of load cycles as described by Lees and Tutumluer [24].

Conversion of settlement to rut depth

Equation (20) was derived from trafficking data on a typical road base aggregate overlying a high plasticity clay subgrade where the surface rutting was largely governed by the subgrade rutting beneath. It would be expected to provide conservative conversions to rut depth for subgrade soils of lower plasticity. Equation (20) would probably provide even more conservative conversions for granular subgrades or where surface rutting were governed by aggregate layer deformations since these materials compress more readily and would be less prone to the heave that causes rutting to accumulate faster than settlement.

The derivation of relationships between settlement and rut depth for specific soil types would require trafficking trials on those specific materials with measurement of both settlement and rut depth accumulation.

Deformation accumulation (ratcheting) relationship

Equation (23) was derived from trafficking data on typical road base aggregates overlying high plasticity clay subgrades where the surface rutting was largely governed by the subgrade rutting beneath. It would be expected to provide conservative rut depth predictions for subgrade soils of lower plasticity. It may provide reasonable predictions of rut depth in alternative aggregate types since the change in shear strength of the aggregate layer is taken into account in the calculation of M_T, but this would need further testing to be confirmed. Ratcheting deformation accumulation in granular subgrade soils would not be expected unless they had liquefied.

Conclusions

A new design method for unpaved roads to calculate the required aggregate layer thickness to avoid excessive rutting at both the road surface and subgrade surface has been proposed in this paper. Its explicit treatment of tyre size and wheel load means that it should be applicable to a wide range of cases from heavy haul roads to lightly trafficked local roads. Furthermore, its analytical basis using well-established soil mechanics principles such as bearing capacity and mobilised strength design has provided a framework for the method's application to a wide range of aggregate and subgrade soil types, including low-quality or recycled aggregates as well as those mechanically stabilised by geogrid.

New soil types require only the common soil parameters, e.g. shear strength φ' or s_u and unit weight in order to obtain approximate designs. Their accuracy can be improved by undertaking well-executed laboratory or in situ tests to establish the hyperbolic relationship between mobilised strength and permanent strain and cyclic tests to establish the α value for the deformation accumulation function. The reliability of design equations for new soil types would be improved significantly with full-scale trafficking and cyclic plate load tests on unpaved roads of those materials but, being a mechanistic method, it does not require the number of full-scale tests that an empirical method requires. A further advantage of the explicit treatment of tyre size is the easier direct comparison between cyclic plate load and trafficking trial performance.

The proposed method is thought to be the first to calculate aggregate layer deformation accumulation as well as subgrade deformation accumulation, thereby allowing output of both subgrade and surface rut depth. In many cases, subgrade rutting is the more serious because it can lead to water ponding on low-permeability soils and hence degradation of strength as well as being more difficult to identify and repair. Furthermore, adoption of a hyperbolic relationship between bearing capacity mobilisation and permanent deformation has widened the scope of design performance levels from as low as a few millimetres of rut depth to about 125 mm. Existing design methods consider either a narrow range or only a single rut depth value.

The main part of the proposed design method is based on shakedown patterns of deformation accumulation for which the bearing capacity mobilisation ratio is restricted to 0.5 in the subgrade to prevent ratcheting failure. However, an additional part allowing higher mobilisation ratios and a linear deformation accumulation pattern was proposed to allow more economical designs in temporary roads with up to 2,000 axle passes.

The equations of the proposed design method have been calibrated using full-scale cyclic plate load and channelised trafficking tests, so can be considered valid for the range of conditions covered in those tests and described in this paper.

The proposed method would benefit from further testing and research for a wider range of conditions, particularly for new soil types. The vast majority of existing test data includes only high-quality road base aggregates and plastic clay subgrades. The effects of wheel wander could also be added.

CRediT authorship contribution statement

A.S. Lees: Conceptualization, Methodology, Validation, Formal analysis, Writing – original draft, Writing – review & editing, Visualization. **J. Han:** Methodology, Writing – original draft, Writing – review & editing.

Declaration of competing interest

The authors declare that they have no known competing financial interests or personal relationships that could have appeared to influence the work reported in this paper.

Data availability

Data will be made available on request.

References

[1] GY. Baladi LE. Vallejo T. Goitom Normalized characterization model of pavement materials, *Properties of Flexible Pavement Materials* ASTM STP 807 (ed. JJ Emery) 1983 55 64.

[2] Black WPM (1979) The strength of clay fill subgrades: its prediction in relation to road performance, TRRL Laboratory Report 889.

[3] BRE. BR470 Working platforms for tracked plant. BRE: Watford; 2004.

[4] Brown SF. Soil mechanics in pavement engineering. Géotechnique 1996;46(3):383–426.

[5] BSI Methods of test for soils for civil engineering purposes – Part 9: In-situ tests. BS 1377-9:1990. BSI, London.

[6] Chaddock BCJ. Deformation of road foundations with geogrid reinforcement, Research Report 140. Crowthorne, UK: Transport and Road Research Laboratory; 1988.

[7] Chang L, Zhang W, Ma Y, Shen P, Han J. Laboratory investigation of boundary effect on pressure-settlement behavior of foundation soil with limited thickness involving geosynthetics. Geotext Geomembr 2020;48(5):747–54.

[8] Collins IF, Boulbibane M. Geomechanical analysis of unbound pavements based on shakedown theory. J Geotech Geoenviron Eng 2000;126(1):50–9.

[9] J. Cook M. Dobie D. Blackman The development of APT methodology in the application and derivation of geosynthetic benefits in roadway design, in The Roles of Accelerated Pavement Testing in Pavement Sustainability, (JP Aguiar-Moya et al (eds.)) 2016 257 275.

[10] Cote BM. Performance comparison of mechanical and chemical stabilization of undercut subgrades. NC: North Carolina State University, Raleigh; 2009. MSc thesis.

[11] Cuelho E, Perkins S, Morris Z. Relative operational performance of geosynthetics used as subgrade stabilization, FHWA/MT-14-002/7712-251. Montana Department of Transportation; 2014.

[12] De Beer M, Maina JW, van Rensburg Y, Greben JM. Toward using tire-road contact stresses in pavement design and analysis. Tire Sci Technol 2012;40(4):246–71.

[13] Duncan JM, Chang C-Y. Nonlinear analysis of stress and strain in soils. Journal of Soil Mechanics and Foundations Division ASCE 1970;96(5):1629–53.

[14] Garcia-Rojo R, Herrmann HJ. Shakedown of unbound granular material. Granul Matter 2005;7(2–3):109–18.

[15] Giroud JP, Han J. Design method for geogrid-reinforced unpaved roads. I. Development of design method. J Geotech Geoenviron Eng 2004;130(8):775–86.

[16] Giroud JP, Noiray L. Geotextile-reinforced unpaved road design. J Geotech Eng 1981;107(9):1233–54.

[17] CR. Gonzalez WR. Barker A. Bianchini Reformulation of the CBR Procedure, Report I: Basic Report, US Army Corps of Engineers, ERDC/GSL TR-12-16 2012.

[18] P.Jenkins IA. Kerr The strength of well graded cohesive fills, Ground Engineering, March 1998 38 41.

[19] Khoueiry N. Study of granular platforms behaviour over soft subgrade reinforced by geosynthetics: experimental and numerical approaches. University of Lyon; 2020. PhD thesis,.

[20] J. Klopmaker L. Vollmert A. Emersleben Geogrids used as subgrade stabilization - experience from large scale field trials, 3rd Pan-American Conference on Geosynthetics, *GeoAmericas 2016* 10 13 April, Miami Beach.

[21] Lees AS. The bearing capacity of a granular layer on clay. Proceedings of the Institution of Civil Engineers - Geotechnical Engineering 2020;173(1):13–20.

[22] Lees AS, Kelly RB. Railway formation design by elasto-plastic FEM mechanistic-empirical approach. Transp Geotech 2023;39:100955.

[23] AS. Lees WJ. Robinson M. Wayne J. Han An investigation of tyre contact area on unbound aggregate, *Proceedings of the 76th Canadian Geotechnical Conference, Saskatoon, 1-4 October.* 2023.

[24] Lees AS, Tutumluer E. A shakedown deformation accumulation function for cyclic triaxial tests on a range of soil types. Under review; 2024.

[25] Lefebvre G, LeBoeuf D, Demers B. Stability threshold for cyclic loading of saturated clay. Can Geotech J 1989;26(1):122–31.

[26] Li D. Railway track granular layer thickness design based on subgrade performance under repeated loading. Amherst: University of Massachusetts; 1994. PhD dissertation,.

[27] Little PH. The design of unsurfaced roads using geosynthetics. University of Nottingham; 1992. PhD thesis,.

[28] Loukidis D, Salgado R. Bearing capacity of strip and circular footings in sand using finite elements. Comput Geotech 2009;36(5):871–9.

[29] Mandel J, Salencon J. Force portante d'un sol sur une assige rigide (étude théorique). Géotechnique 1972;22:79–93.

[30] Meyerhof GG. Ultimate bearing capacity of footings on sand layer overlying clay. Can Geotech J 1974;11(2):223–9.

[31] CL. Monismith N. Ogawa CR. Freeme Permanent deformation characteristics of subgrade soils due to repeated loading, *Transportation Research Record* **537**: 1-17. Palmeira EM and Antunes LGS (2010). Large scale tests on geosynthetic reinforced unpaved roads subjected to surface maintenance, *Geotextiles and Geomembranes* **28** 1975 547 558.

[32] Palmeira EM, Antunes LGS. Large scale tests on geosynthetic reinforced unpaved roads subjected to surface maintenance. Geotext Geomembr 2010;28(6):547–58.

[33] OJ. Porter Accelerated Traffic Test at Stockton Airfield Stockton, California (Stockton Test No. 2), Corps of Engineers Sacramento District, Department of the Army. 1949.

[34] Powell WD, Potter JF, Mayhew HC, Nunn ME. The structural design of bituminous roads, TRRL Laboratory Report 1132. Crowthorne, UK: Transport and Road Research Laboratory; 1984.

[35] Pycko S, Maier G. Shakedown theorems for some classes of nonassociative hardening elasticplastic material models. Int J Plast 1995;11(4):367–95.

[36] Sangrey DA. The behaviour of soils subjected to repeated loading. USA: Cornell University; 1968. PhD thesis).

[37] Terzaghi K. Theoretical soil mechanics. New York: John Wiley and Sons; 1943.

[38] Thompson RJ, Peroni R, Visser AT. Mining haul roads theory and practice. 1st edition. Leiden, The Netherlands: CRC Press; 2019.

[39] Tingle JS, Jersey SR. Cyclic plate load testing of geosynthetic-reinforced unbound aggregate roads. Transp Res Rec 2005;1936(1):60–9.

[40] Tingle JS, Webster SL. Corps of engineers design of geosynthetic-reinforced unpaved roads. Transp Res Rec 2003;1849:193–201.

[41] Vardanega PJ, Bolton MD. Strength mobilization in clays and silts. Can Geotech J 2011;48:1485–503.

[42] Watts GRA, Blackman DI, Jenner CG. The performance of reinforced unpaved sub-bases subjected to trafficking. Third European Geosynthetics Conference, Munich 2004;1:261–6.

[43] D. White Laboratory test results, Inios Geotechnics confidential report. 2019.

[44] Yang X, Han J, Pokharel SK, Manandhar C, Parsons RL, Leshchinsky D, et al. Accelerated pavement testing of unpaved roads with geocell-reinforced sand bases. Geotext Geomembr 2012;32:95–103.

[45] Zergoun M, Vaid YP. Effective stress response of clay to undrained cyclic loading. Can Geotech J 1994;31:714–27.